Synthesis and in Vitro Antifolate Activity of Rotationally Restricted Aminopterin and Methotrexate Analogues

Andre Rosowsky,* Ronald A. Forsch, and Joel E. Wright

Dana-Farber Cancer Institute and Department of Biological Chemistry and Molecular Pharmacology, Harvard Medical School, Boston, Massachusetts 02115

Received June 25, 2004

Heretofore unknown analogues of aminopterin (AMT) and methotrexate (MTX) in which free rotation of the amide bond between the phenyl ring and amino acid side chain is prevented by a CH_2 bridge were synthesized and tested for in vitro antifolate activity. The K_i of the AMT analogue (**9**) against human dihydrofolate reductase (DHFR) was 34 pM, whereas that of the MTX analogue (**10**) was 2100 pM. Both compounds were less potent than the parent drugs. However, although the difference between AMT and MTX was <2-fold, the difference between **9** and **10** was 62-fold, suggesting that the effect of N^{10}-methyl substitution is amplified in the bridged compounds. The K_i values of **9** and **10** as inhibitors of [^{3}H]MTX influx into CCRF−CEM human leukemia cells via the reduced folate carrier (RFC) were 0.28 and 1.1 μM, respectively. The corresponding K_i and K_t values determined earlier for AMT and MTX were 5.4 and 4.7 μM, respectively. Thus, in contrast to its unfavorable effect on DHFR binding, the CH_2 bridge *increased RFC binding*. In a 72 h growth assay with CCRF−CEM cells, the IC_{50} valuess of **9** and **10** were 5.1 and 140 nM, respectively, a 27-fold difference that was qualitatively consistent with the observed combination of weaker DHFR binding and stronger RFC binding. Although rotationally restricted inhibitors of other enzymes of folate pathway enzymes have been described previously, **9** and **10** are the first reported examples of DHFR inhibitors of this type.

Introduction

Several examples of analogues of folic acid (**1**) in which the B-ring, 9,10-bridge, or pABA moiety is modified, and in addition the glutamyl nitrogen is tethered to the ortho position of the phenyl ring via a CH_2 bridge to prevent free rotation of the amide bond, have been described in the literature. Specifically they include the 2-methylquinazolin-4(3*H*)-one **2**,[1] the 3-methylbenzo[*f*]quinazolin-1(2*H*)-one **3**,[2] the 2-aminopyrido[2,3-*d*]pyrimidin-4(3*H*)-ones **4**,[3] **5**,[4] and **6**,[4] the 2-aminopyrrolo[2,3-*d*]pyrimidin-4(3*H*)-one **7**,[3] and the 2-aminothieno[2,3-*d*]pyrimidin-4(3*H*)-one **8**.[3] Compounds **2** and **3** were designed as inhibitors of the enzyme thymidylate synthase (TS), compounds **5** and **6** as conformationally restricted analogues of (6*R*,6*S*)-2,4-diamino-5-deaza-5,6,7,8-tetrahydrofolate (DDATHF, LY237147), an inhibitor of the key purine pathway enzyme glycinamide ribotide formyltransferase (GARFT), and compound **7** as an analogue of the novel multitargeted antifolate pemetrexed (MTA, LY231514), whose polyglutamates are potent inhibitors not only of TS and GARFT but also to a lesser extent dihydrofolate reductase (DHFR). The structures of **1**−**8** are shown in Figure 1.

Rotationally restricted inhibitors of a third key enzyme of folate metabolism, dihydrofolate reductase (DHFR), have, until now, not been described in the literature. In the present paper, we report the synthesis of compounds **9** and **10**, which may be viewed as rotationally restricted analogues of the classical DHFR inhibitors aminopterin (AMT, **11**) and methotrexate (MTX, **12**), respectively. Also reported are initial data on the in vitro antifolate activity of these compounds in comparison with AMT and MTX. To our knowledge, **9** and **10** are the first examples of *2,4-diamino* antifolates with a rotationally restricted glutamate side chain.

Chemistry

The synthesis of **9** began with methyl 2-(bromomethyl)-4-nitrobenzoate (**13**), which was converted to the key lactam **15**[1,4] as summarized in Scheme 1. This was followed by condensation with 2,4-diamino-6-bromomethylpteridine (**16**)[5] and saponification of the resulting ester **17** with $Ba(OH)_2$. Although it proved expedient to run through the sequence from **13** to **17** with only partial purification of the intermediates **14** and **15**, the end product **9** was obtained in very pure state by a two-stage process consisting of preparative HPLC on C_{18} silica gel followed by ion-exchange chromatography on DEAE−cellulose. Lyophilization of appropriately pooled fractions afforded **9** as a yellow powder whose microchemical analysis showed it to be a hydrated partial ammonium salt and whose 200 MHz ^{1}H NMR spectrum in d_6-DMSO solution showed the requisite features including a pair of doublets centered at δ 4.25 and δ 4.49 for the diastereotopically nonequivalent CH_2 protons of the isoindolinone ring. Likewise consistent with structure of **9** were a doublet at δ 7.39 and a singlet at δ 8.39, which could be assigned to the isoindolinone H-7 and the pteridine H-7 protons, respectively. The isoindolinone H-4 and H-6 aromatic protons gave rise to a poorly resolved A_2B_2 pattern that was partially obscured by a broad singlet corresponding to one of the NH_2 groups. The overall yield of **9** from the amino lactam **15** was 28%.

For the synthesis of the N^{10}-methyl analogue **10**, we initially considered making the previously unknown

* Corresponding author. Phone: 617-632-3117. Fax: 617-632-2410. E-mail: andre_rosowsky@dfci.harvard.edu.

10.1021/jm040122s CCC: $27.50
Published on Web 12/02/2004

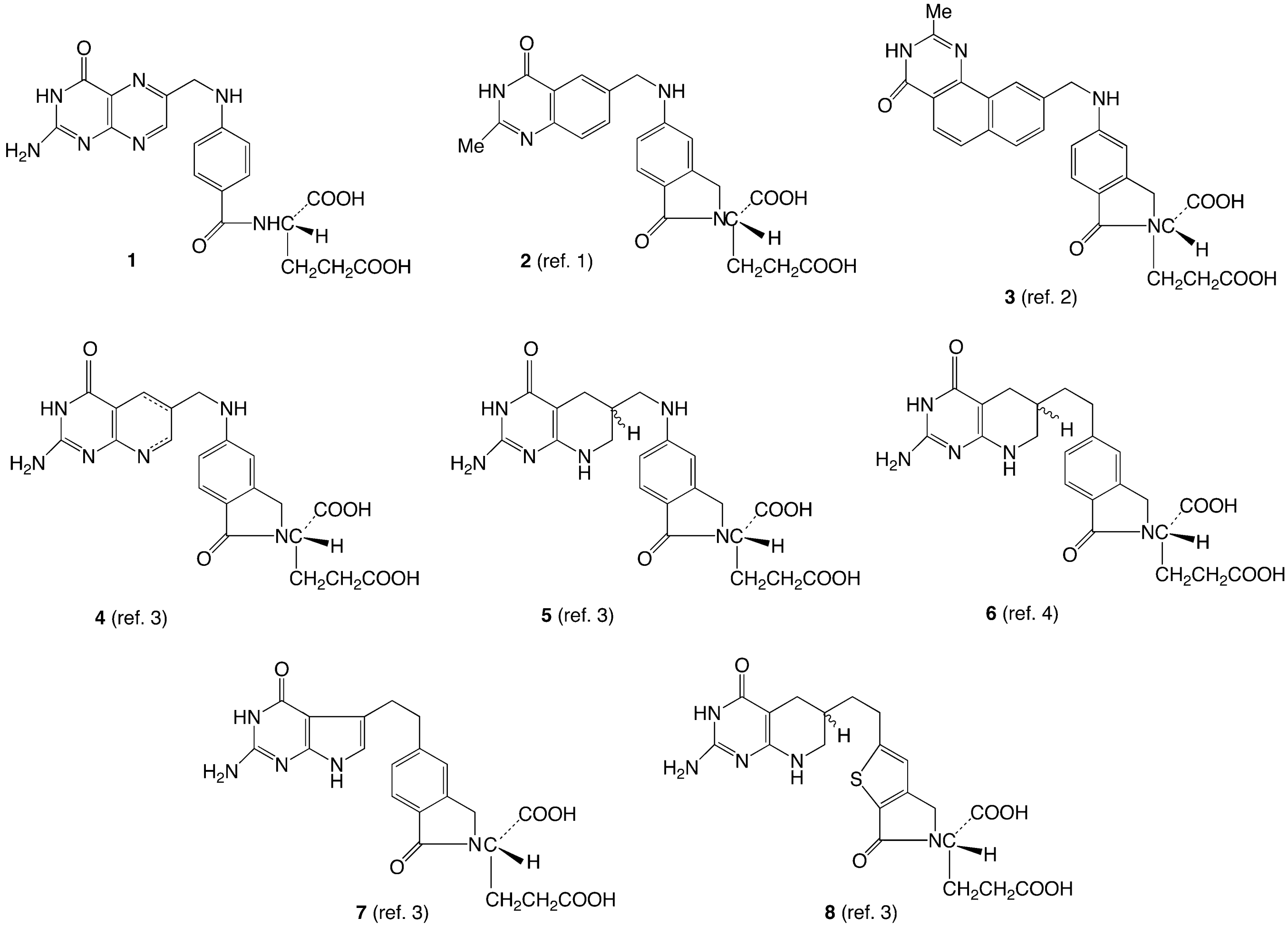

Figure 1. Structures of folic acid (**1**) and its previously reported analogues **2**–**8** with a rotationally restricted side chain amide bond.

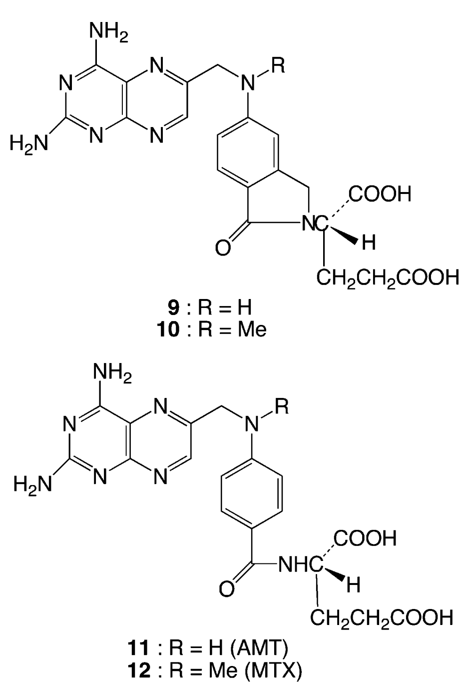

Figure 2. Structures of aminopterin (AMT, **9**), methotrexate (MTX, **10**), and their analogues **11** and **12** with a rotationally restricted side chain amide bond.

N-methylamino lactam **18** by direct methylation of **15**. However, given the separation problem and resultant low yield of monomethylated product likely to be encountered in the reaction of **15** with methyl iodide, we chose instead to start with commercially available 4-bromo-2-methylbenzoic acid (**19**) and take advantage of the elegant Pd^0 catalyzed amination procedure recently developed by Hartwig and co-workers.[6] As shown in Scheme 1, **19** was esterified ($SOCl_2$/MeOH), and the resulting ester **20** was condensed with *N*-benzylmethylamine in the presence of tris(dibenzylideneacetone)-dipalladium(0) (Pd_2dba_3), tri-*tert*-butylphosphine, and cetyltrimethylammonium hydroxide as a phase transfer catalyst in a well-stirred mixture of aqueous NaOH and toluene. This afforded **21**, which was then converted stepwise to **22** and **23** by catalytic hydrogenolysis (H_2/Pd–C) and acylation with trifluoroacetic anhydride in pyridine, respectively. Bromination of the methyl group with *N*-bromosuccinimide (NBS) and benzoyl peroxide, followed by reaction of the crude bromide **24** with diethyl L-glutamate and removal of the trifluoroacetyl group with K_2CO_3 in aqueous EtOH, afforded the methylamino lactam **18**. Condensation of **18** and **16**, followed by saponification using $Ba(OH)_2$, yielded the diester **25** and diacid **10**, respectively. The yield of **10** based on **18** was 48%. In contrast to **9**, purification of **10** was accomplished by preparative HPLC on C_{18} silica gel without need of additional ion-exchange chromatography. Microchemical analysis indicated that in this case the product contained approximately two molecules

Scheme 1

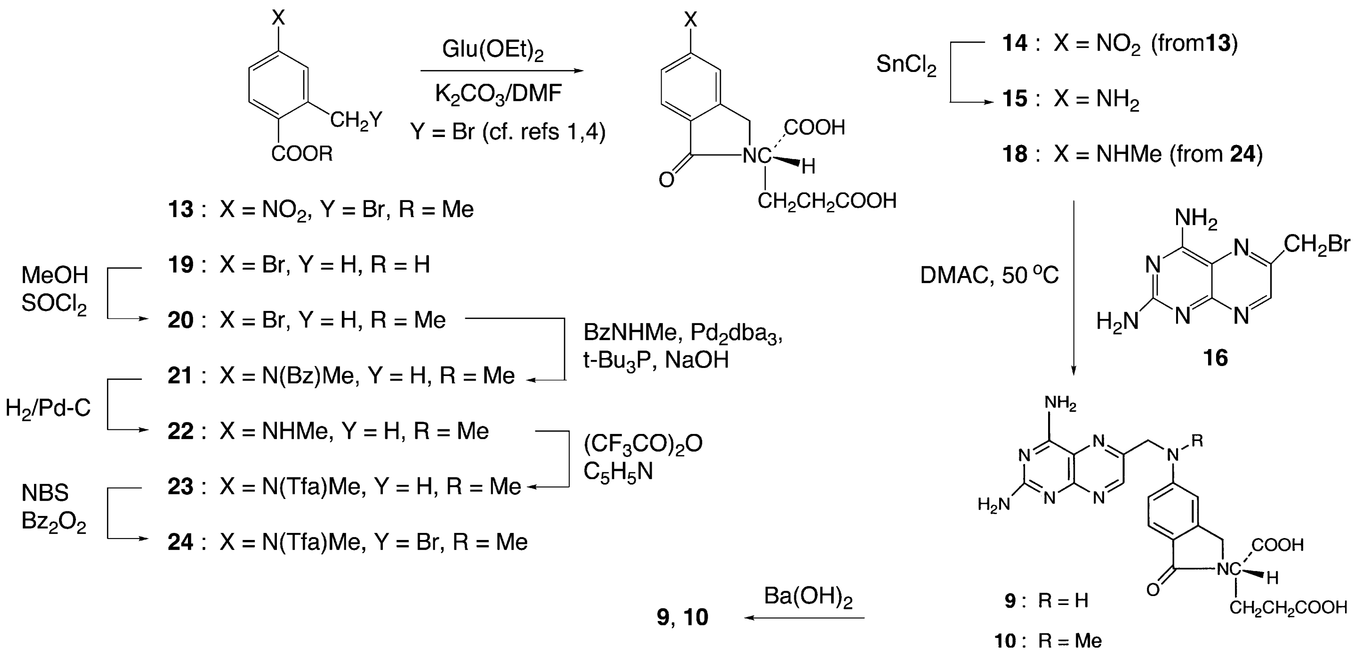

of water but no ammonia. Ultraviolet spectra of **9** and **10** showed same type of UV shift as was reported originally in MTX versus AMT[7] and has since been observed in other cases involving replacement of the pteridine by a different 2,4-diaminoheterocyclic ring system[8,9] or the glutamate side chain by another amino acid.[10,11] The likely reason for this difference between N^{10}-methyl and N^{10}-unsubstituted AMT and MTX analogues is that the methyl group enhances the basicity of the nitrogen, thereby favoring delocalization of the lone pair of electrons into the benzoyl moiety via the coplanar resonance structures **9a** and **10a**.

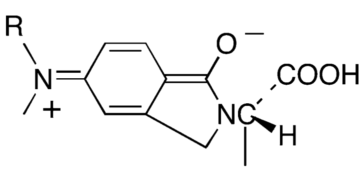

9a: R = H
10a: R = Me

The ^{1}H NMR spectrum of **10** was different from that of **9** in two notable respects. Although the isoindolinone CH_2 group of **9** gave rise to a pair of well-resolved one-proton doublets, the spectrum of **10** contained only a two-proton singlet, suggesting a smaller degree of nonequivalence. Consistent with the ring-closed structure of **10** was the finding that the isoindolinone CH_2 protons gave a ^{1}H NMR signal (δ 4.38) in the same general region as in **9**, whereas if ring opening had occurred during saponification then the CH_2 group next to the nonacylated nitrogen would presumably be further upfield. Furthermore, although the exchangeable peak for one of the NH_2 groups in **9** overlapped the H-4 and H-6 protons, in the spectrum of **10** this NH_2 group appeared to be shifted downfield so that it overlapped the H-7 proton. Overall, the ^{1}H NMR data suggested a subtle perturbation of the magnetic environment in both the phenyl and isoindolinone ring in comparison with **9**.

Formation of **18** from **24** and diethyl l-glutamate was found to yield two minor byproducts that had to be carefully removed by chromatography in order to avoid carrying them to the next step. From the ^{1}H NMR spectrum, it appears that these byproducts were the lactam methyl and ethyl esters **26** and **27**, arising from **24** by nucleophilic attack of the glutamate amino group on the $BrCH_2$ group, ring closure onto the γ-glutamyl carbon, and partial transesterification of the aromatic CO_2Me group during removal of the *N*-trifluoroacetyl group with EtOH as the solvent. Whereas the chemical shift for the CH_2 group in isoindoline **15** was part of a complex multiplet at δ 4.1−4.6[4] and this feature was replicated in the spectrum of **18**, the ^{1}H NMR spectrum of the putative byproducts **26** and **27** displayed a clearly separated CH_2 singlet downfield at δ 5.13, in agreement with the presence of an electron-withdrawing ester group at the ortho position of the phenyl ring. Although analogous byproducts could have formed also during the earlier synthesis of **15** from **13**,[4] this possibility was not investigated.

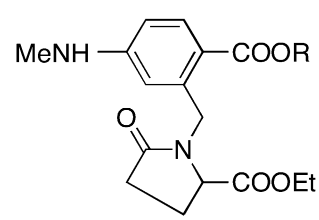

26 : R = Me
27 : R = Et

An alternative route to **9** that we also explored began with the condensation of **15** with 2-amino-5-bromomethylpyrazine-3-carbonitrile (**28**) to form the substituted pyrazine **29**. This was followed by ring closure with guanidine and saponification with NaOH (Scheme 2). However the bioassay data for this product (Table 1) indicated that racemization had probably taken place at the glutamyl α-carbon, just as Mautner and co-

Scheme 2

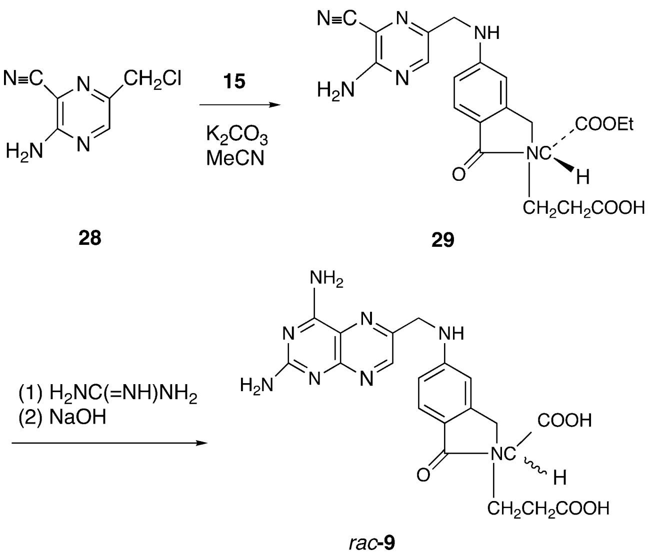

Table 1. In Vitro Antifolate Activity of Rotationally Restricted AMT and MTX Analogues[a]

cmpd	DHFR K_i (pM)	influx K_i (μM)	growth IC_{50} (nM, 72 h)
9	34 ± 3.0	0.28 ± 0.10	5.1 ± 0.25
rac-**9**	77 ± 1.2	0.53 ± 0.03	8.4 ± 0.7
10	2100 ± 200	1.1 ± 0.11	140 ± 5.0
AMT (**11**)	3.7 ± 0.35	5.4 ± 0.09	4.4 ± 0.10
MTX (**12**)	4.8 ± 0.45	4.7 ± 1.3 (K_t)	14 ± 2.6

[a] All of the numbers are rounded off to two significant figures and are the means ± SD ($n \geq 3$). Data for AMT and MTX are taken from refs 13b and 14. The racemic nature of *rac*-**9** obtained via Scheme 2 is indicated by its roughly 2-fold lower potency in all three assays relative to **9** obtained via Scheme 1.

workers[12a,b] had observed earlier in their synthesis of aminopterin and 10-thiaaminopterin from **26**. Although we had hoped that the absence of an ionizable hydrogen on the amide group of **27** might prevent such racemization, this turned out not to be the case.

Antifolate Activity. Because there was no information in the literature on the effect that a CH_2 bridge might have on the biological activity of AMT and MTX, the ability of **9** and **10** to bind to human DHFR was assessed spectrophotometrically as described previously,[13] and the K_i values were compared with those that we had obtained earlier for AMT and MTX. As shown in Table 1, the K_i of **9** was 34 ± 3.0 pM and that of **10** was 2100 ± 200 pM. Both compounds were less potent than their nonbridged counterparts, but there was an unexpected difference between them in that **10** was 440 times less potent than MTX (K_i = 4.8 ± 0.45 pM), whereas the difference in K_i between **9** and AMT (K_i = 3.7 ± 0.35 pM) was only 9-fold. Thus. N^{10}-methylation appeared to produce a 62-fold decrease in binding when rotation about the side chain amide bond was blocked by a CH_2 bridge to the ortho position of the phenyl ring, but almost no decrease was observed in the absence of a bridge. This suggests that, for optimal binding to the enzyme, the amide bond of both MTX and AMT may need to be able to point further out of the plane of the phenyl ring than is possible when the amide nitrogen is part of a fused five-membered ring and that this requirement is more easily met when N^{10} is unsubstituted. However, it cannot be ruled out that the observed DHFR binding difference between the bridged and the nonbridged compounds reflects not only the inability of the amide bond to rotate freely but also the fact that the phenyl ring is 6′-substituted. A comparative X-ray crystallographic analysis of the orientation of the amide carbonyl oxygen atom relative to the α-COOH group in the bridged and nonbridged compounds in ternary complexes with DHFR and NADPH would shed light on this complex issue and is currently planned.

In addition to the effect on DHFR binding, it was equally of interest to assess whether the introduction of a CH_2 bridge to restrict free rotation of the side chain amide bond of AMT and MTX would have a deleterious effect on transport via the reduced folate carrier (RFC), just as it does on DHFR binding. Thus, we determined the K_i of **9** and **10** inhibitors of [^{3}H]MTX influx into CCRF−CEM human leukemic lymphoblasts over a 60-s period as previously described.[14] As shown in Table 1, the K_i of **9** was 0.28 ± 0.10 μM, whereas that of **10** was 1.1 ± 0.11 μM, a 4-fold difference again favoring the N^{10}-unsubstituted analogue. The K_i value that we had obtained earlier for AMT was 5.4 ± 0.09 μM, and the K_t for MTX (equivalent to the K_i in this case) was 4.7 ± 1.3 μM (Table 1). Thus, **9** and **10** were both able to bind better to the RFC than their nonbridged counterparts. Moreover, rotational restriction of the side chain amide bond appeared to have the opposite effect on RFC binding than on DHFR binding. This suggests that, in contrast to DHFR binding, a coplanar arrangement between the side chain amide bond and the phenyl ring may be favorable where RFC binding is concerned. The low K_i of **9** was gratifying, because until now the only DHFR inhibitors we had found to give a K_i of <0.4 μM in this assay were analogues of N^{α}-(4-amino-4-deoxypteroyl)-N^{δ}-hemiphthaloyl-L-ornithine (PT523) in which the B-ring (5- or 5,8-dideaza) or 9,10-bridge (10-deaza or 5,8,10-trideaza) are modified but the amide bond is not locked in place. However, whether restricted rotation of the amide bond would also promote RFC binding when the side chain is N^{δ}-hemiphthaloyl-L-ornithine remains to be determined.

With the knowledge that **9** and **10** were weaker DFHR inhibitors than AMT and MTX, but could bind somewhat better to the RFC, it was of interest to assess their ability to inhibit cell growth in culture under the standardized conditions routinely used in our laboratory in the past.[15] As shown in Table 1, the IC_{50} values of **9** and **10** against CCRF−CEM cells during 72 h of exposure were 5.1 ± 0.25 and 140 ± 5.0 nM, as compared with previously determined values of 4.4 ± 0.10 and 14 ± 2.6 nM for AMT and MTX, respectively. It thus appeared that the increase in RFC binding of **9** relative to AMT was able to approximately offset its decrease in DHFR binding, whereas in the case of **10** versus MTX the modest gain in RFC binding was not enough to offset a much larger decrease in DHFR binding.

As indicated in Table 1, the K_i values for DHFR inhibition and [^{3}H]MTX influx as well as the IC_{50} value for cell growth inhibition were all ca. 2-fold higher for the product obtained via Scheme 2 than for the one obtained via Scheme 1. We interpreted these results to mean that significant racemization had taken place at the α-carbon under the highly basic conditions of guanidine cyclization and moreover that essentially all of the the biochemical and biological activity was provided by the diastereomer with the "natural" configuration. In the classic work of Mautner and coworkers[12a,b] on the synthesis of AMT analogues by this method, racemization was inferred from the absence of optical activity in the product. The present findings, based on in vitro biochemical and biological evidence rather than physical data, complement the earlier study and confirm that heating with guanidine must be avoided if a chiral carbon is already present.[16]

The lower degree of proportionality between DHFR binding, RFC binding, and cytotoxicity in the case of **10** versus **9** presumably reflects (a) differences in substrate activity of the two compounds for γ-folylpolyglutamate synthetase (FPGS),[17] (b) the nature of the product(s) of the FPGS reaction and their relative ability to inhibit DHFR,[18] (c) the ability of γ-folylpolyglutamate hydrolase (FPGH) to cleave the γ-diglutamyl derivatives back to the original drug,[19] and (d) the possible substrate activity of each species for one or more of the multidrug resistance proteins (MRPs) that have recently been shown to mediate MTX efflux.[20] A detailed analysis of the pharmacodynamics of **9** and **10** to address these complex interdependent variables would be of interest but was beyond the scope of this study.

Experimental Section

2-*S*-[5-[(2,4-Diaminopteridin-6-yl)methylamino]-2,3-dihydro-1-oxo-2(1*H*)-isoindolyl]glutaric Acid (9). Compound **15** (200 mg, 0.58 mmol, as the crude product of reduction of **14** with $SnCl_2$)[4] and **16**·HBr (212 mg, 0.58 mmol, assumed to be solvated with *i*-PrOH as reported in the literature)[5] were dissolved in DMAC (5 mL), and the solution was heated at 50 °C for 7 days. The reaction mixture, containing diester **17**, was diluted with 95% EtOH (30 mL) and H_2O (20 mL), and solid $Ba(OH)_2{\cdot}8H_2O$ (1.26 g, 4.0 mmol) was added. The mixture was then stirred at room temperature for 3 days, and a solution of $(NH_4)_2CO_3$ (384 g, 4.0 mmol) in H_2O (5 mL) was added. After the solution was stirred for another 10 min, the insoluble $BaCO_3$ was filtered and the filter cake was washed with H_2O. The filtrate was concentrated by rotary evaporation until most of the EtOH was removed, and a small amount of insoluble material was filtered off. The final pH of the filtrate was ca. 8.0. Analytical HPLC (C_{18} silica gel, 5% MeCN in 0.1 M NH_4OAc, pH 7.4, 1.0 mL/min) showed a major peak eluting at 10 min along with a slower peak at >20 min, with each peak being detectable at both 280 and 370 nm. A fast peak (2 min) was also seen at 280 nm but not 370 nm. The entire sample was then purified on a preparative scale using the same eluent buffer except that the MeCN concentration was initially decreased to 3% and then raised to 5% as the main peak began to elute. Appropriately pooled eluates were concentrated by rotary evaporation followed by freeze-drying. The residue was taken up in 10% NH_4OH, the solution was filtered to remove a small amount of adventitious C_{18} silica gel, and 10% AcOH was added to reprecipitate the product. The resulting solid was filtered and subjected to final purification by ion-exchange chromatography on DEAE−cellulose (HCO_3^{-1} form, 1.5 cm × 19 cm, 0.4 M NH_4HCO_3). Appropriately pooled fractions were again concentrated and freeze-dried to obtain **9** as a yellow powder (81 mg, 28%). Mp: >250 °C. IR (KBr) ν: 3350, 3200, 1645, 1615, 1540, 1505, 1450, 1405, 1385, 1290, 1260, 1225, 1130−1100br, 995, 810, 770, 690, 620 cm^{-1}. UV λ_{max} (0.05 M phosphate buffer, pH 7.4): 223 nm (ϵ 23 700), 259 (24 000), 285 (23 300), 370 (8000). ^{1}H NMR (DMSO-d_6): δ 2.49 (m, 4H, β- and γ-CH_2), 4.25 (d, 1H, isoindolinone H-3α), 4.49 (m, 4H, CH_2NH, α-CH, isoindolinone H-3β), 6.57 (s, 2H, NH_2), 6.80 (4H, NH_2, isoindolinone H-4 and H-6), 7.39 (d, J = 8 Hz, 1H, isoindolinone H-7), 8.70 (s, 1H, pteridine H-7). Anal. ($C_{20}H_{20}N_8O_5{\cdot}2.75H_2O$) C, H, N.

2-*R,S*-[5-[(2,4-Diaminopteridin-6-yl)methylamino]-2,3-dihydro-1-oxo-2(1*H*)-isoindolyl]glutaric Acid (*rac*- 9). Metallic Na (37 mg, 1.61 mmol) was dissolved in EtOH (10 mL), solid guanidine hydrochloride (152 mg, 1.6 mmol) was added, and after 5 min of being swirled, the mixture was added to the ethanolic solution of **29** obtained after workup of the reaction of **15** with **28** (cf. Supporting Information). The reaction mixture was stirred under reflux for 20 h, then cooled to room temperature, treated with 1 M NaOH (5 mL), stirred for 5 min, and evaporated under reduced pressure. The residue was subjected to preparative HPLC (C_{18} silica gel, 3.3% MeCN in 0.1 M NH_4OAc, pH 6.9, 1.0 mL/min), and appropriately pooled fractions (R_f = 14 min, dual detection at 280 and 370 nm) were concentrated by rotary evaporation followed by freeze-drying. The residue was taken up in dilute NH_4OH, a small amount of insoluble material was filtered off, and 10% AcOH was added to reprecipitate the product. Freeze-drying of the entire acidified mixture afforded *rac*-**9** as a yellow powder (124 mg, 23%) whose IR spectrum, ^{1}H NMR spectrum, and HPLC elution time from the C_{18} silica gel matched those of **9** obtained from **14** and **16**·HBr as described above. Anal. ($C_{20}H_{20}N_8O_5{\cdot}0.25NH_3{\cdot}4.5H_2O$) C, H, N.

2-*S*-[5-[*N*-(2,4-Diaminopteridin-6-yl)methyl)-*N*-methylamino]-2,3-dihydro-1-oxo-2(1*H*)-isoindolyl]glutaric Acid (10). From purified **18**, prepared from **22**−**24** (cf. Supporting Information), this compound was obtained via **25** by essentially the same procedure as **9** except that the reaction mixture was heated at 50 °C for only 3.5 days. After removal of the $BaCO_3$, the EtOH was removed from the aqueous EtOH filtrate by rotary evaporation, a small amount of fine white solid was filtered off, the filtrate was allowed to stand at room temperature overnight, and an additional small quantity of fine solid was removed. Analytical HPLC (C_{18} silica gel, 8% MeCN in 0.1 M NH_4OAc, pH 7.4) showed a major peak eluting at 13 min, along with two faster-moving impurities. For preparative HPLC, the initial MeCN concentration was reduced to 4% and was increased to 8% as the main peak began to elute. Appropriately pooled eluates were concentrated and freeze-dried to obtain **10** as yellow solid (75 mg, 48%). Mp: >250 °C. IR (KBr): ν 3340, 3150br, 2920br, 1615, 1560, 1505, 1450, 1405, 1385, 1360, 1300, 1260, 1205 cm^{-1}. UV λ_{max} (0.05 M phosphate buffer, pH 7.4): 226 nm (ϵ 25 800), 258 (25 500), 308 (24 000), 370 (8100). ^{1}H NMR (DMSO-d_6): δ 2.27 (m, 4H, β- and γ-CH_2), 3.38 (s, NMe, overlapping the H_2O peak), 4.38 (s, 2H, isoindolinone H-3), 4.86 (m, 3H, CH_2NMe and α-CH), 6.69 (br s, NH_2), 7.00 (m, 2H, 4-H and 6-H), 7.52 (br s, NH_2, overlapping 7-H, d, J = 8 Hz), 8.65 (s, 1H, 7-H). Anal. ($C_{21}H_{22}N_8O_5{\cdot}2.2H_2O$) C, H, N.

Acknowledgment. This work was supported in part by Grant RO1-CA25394 from the National Cancer Institute, National Institutes of Health, Department of Health and Human Services. The authors are indebted to Ying-Nan Chen for her technical assistance in the transport and cytotoxicity experiments.

Supporting Information Available: Additional experimental details for the synthesis of compounds **20**−**23** from **19**, compound **18** from **23** via **24**, and compound **29** from **15**. This material is available free of charge via the Internet at http://pubs.acs.org.

References

(1) Marsham, P. R.; Jackman, A. L.; Hayter, A. J.; Daw, M. R.; Snowden, J. L.; O'Connor, B. M.; Bishop, J. A. M.; Calvert, A. H.; Hughes, L. R. Quinazoline Antifolate Thymidylate Synthase Inhibitors: Bridge Modifications and Conformationally Restricted Analogues in the C2-Methyl Series. *J. Med. Chem.* **1991**, *34*, 2209−2218.
(2) Pendergast, W.; Dickerson, S. H.; Dev, I. K.; Ferone, R.; Duch, D. S.; Smith, G. K. Benzo[*f*]quinazoline Inhibitors of Thymidylate Synthase: Methyleneamino-Linked Aroylglutamate Derivatives. *J. Med. Chem.* **1994**, *37*, 838−844.

(3) Taylor, E. C.; Jennings, l. D.; Mao, Z.; Hu, B.; Jun, J.-G.; Zhou, P. Synthesis of Conformationally Constrained Glutamate Analogues of the Antitumor Agents DDATHF, LY254155, and LY231514. *J. Org. Chem.* **1997**, *62*, 5392−5403.

(4) Rosowsky, A.; Forsch, R. A.; Null, A.; Moran, R. G. 5-Deazafolate Analogues with a Rotationally Restricted Glutamate or Ornithine Side Chain: Synthesis and Binding Interaction with Folylpolyglutamate Synthetase. *J. Med. Chem.* **1999**, *42*, 3510−3519.

(5) Piper, J. R.; Montgomery, J. A. A Convenient Synthesis of Aminopterin and Homologues via 6-(Bromomethyl)-2,4-diaminopteridine Hydrobromide. *J. Med. Chem.* **1974**, *11*, 379−380.

(6) Kuwano, R.; Utsunomiya, M.; Hartwig, J. F. Aqueous Hydroxide as a Base for Palladium-Catalyzed Amination of Aryl Chlorides and Bromides. *J. Org. Chem.* **2002**, *67*, 6479−6486.

(7) Seeger, D. R.; Cosulich, D. B.; Smith, J. M., Jr.; Hultquist, M. E. Analogs of Pteroyl-Glutamic Acid. III. 4-Amino Derivatives. *J. Am. Chem. Soc.* **1949**, *71*, 1753−1758.

(8) Srinivasan, A.; Broom, A. D. Pyridopyrimidines. 12. Synthesis of 8-Deaza Analogues of Aminopterin and Folic Acid. *J. Org. Chem*. **1981**, *46*, 1777−1781.

(9) Temple, C., Jr.; Elliott, R. D.; Montgomery, J. A. Pyrido[2,3-*d*]-pyrimidines. Synthesis of the 5-Deaza Analogues of Aminopterin, Methotrexate, Folic Acid, and N^1-Methylfolic Acid. *J. Org. Chem*. **1982**, *47*, 761−764.

(10) Rosowsky, A.; Forsch, R. A.; Freisheim, J. H.; Moran, R. G.; Wick, M. Methotrexate Analogues. 19. Replacement of the Glutamate Side-Chain in Classical Antifolates by l-Homo-cysteic and Cysteic Acids: Effect on Enzyme Inhibition and Antitumor Activity. *J. Med. Chem.* **1984**, *27*, 600−604.

(11) Rosowsky, A.; Forsch, R. A.; Moran, R. G.; Freisheim, J. H. Synthesis and In Vitro Biological Evaluation of β,γ-Methano Analogues of Methotrexate and Aminopterin. *Pteridines* **1990**, *2*, 133−139.

(12) (a) Mautner, H. G.; Kim, Y.-H. The Circular Dichroism of Folic Acid and 10-Thiafolic and the Problem of Racemization in the Synthesis of Analogues of Folic Acid through the Cyclization of Substituted 2-Amino-3-cyanopyrazine. *J. Org. Chem.* **1975**, *40*, 3447−3448. (b) Kim, Y.-H.; Gaumont, Y.; Kisliuk, R. L.; Mautner, H. G. Synthesis and Biological Activity of 10-Thia-10-deaza Analogues of Folic Acid, Pteroic Acid, and Related Compounds. *J. Med. Chem.* **1975**, *18*, 776−780.

(13) (a) Rosowsky, A.; Wright, J. E.; Vaidya, C. M.; Bader, H.; Forsch, R. A.; Mota, C. M.; Pardo, J.; Chen, C. S.; Chen, Y.-N. Synthesis and Potent Antifolate Activity and Cytotoxicity of B-Ring Deaza Analogues of the Nonpolyglutamatable Dihydrofolate Reductase Inhibitor N^α-(4-Amino-4-deoxypteroyl)-N^δ-hemiphthaloyl-L-ornithine (PT523). *J. Med. Chem.* **1998**, *41*, 5310−5319. (b) Wright, J. E.; Yurasek, G. K.; Chen, Y.-N.; Rosowsky, A. Further Studies on the Interaction on Nonpolyglutamatable Aminopterin Analogues with Dihydrofolate Reductase and the Reduced Folate Carrier as Determinants of in Vitro Antitumor Activity. *Biochem. Pharmacol.* **2003**, *65*, 1417−1433.

(14) Wright, J. E.; Vaidya, C. M.; Chen, Y.-N.; Rosowsky, A. Efficient Utilization of the Reduced Folate Carrier in CCRF−CEM Human Leukemic Lymphoblasts by the Potent Antifolate N^α-(4-Amino-4-deoxypteroyl)-N^δ-hemiphthaloyl-L-ornithine (PT523) and Its B-Ring Analogues. *Biochem. Pharmacol.* **2000**, *60*, 41−46.

(15) Rosowsky, A.; Wright, J. E.; Vaidya, C. M.; Forsch, R. A.; Bader, H. Analogues of the Potent Nonpolyglutamatable Antifolate N^α-(4-Amino-4-deoxypteroyl)-N^δ-hemiphthaloyl-L-ornithine (PT523) with Modifications in the Side Chain, *p*-Aminobenzoyl Moiety, or 9, 10-Bridge: Synthesis and In Vitro Antitumor Activity. *J. Med. Chem.* **2000**, *43*, 1620−1634.

(16) On the basis of the findings of Mautner and co-workers[12a,b] and those reported here, there is good reason to believe, as implied by these authors, that prior data reported for DHFR and bacterial growth inhibition by MTX synthesized via this approach were similarly off by a factor of 2. Cf.: Chaykovsky, M.; Rosowsky, A.; Papathanasopoulos, N.; Chen, K. K. N.; Modest, E. J.; Kisliuk, R. L.; Gaumont, Y. Methotrexate Analogues. 3. Synthesis and Biological Properties of Some Side-Chain Altered Analogues. *J. Med. Chem.* **1974**, *17*, 1212−1216.

(17) McGuire, J. J. Antifolate Polyglutamylation in Preclinical and Clinical Antifolate Resistance. In *Antifolate Drugs in Cancer Therapy*; Jackman, A. L., Ed.; Humana: Totowa, NJ, 1999; pp 339−363.

(18) (a) Matherly, L. H.; Voss, M. L.; Anderson, L. A.; Fry, D. W.; Goldman, I. D. Enhanced Polyglutamation of Aminopterin Relative to Methotrexate in the Ehrlich Ascites Tumor Cell In Vitro. *Cancer Res.* **1985**, *45*, 1073−1078. (b) Kumar, P.; Kisliuk, R. L. Gaumont, Y.; Freisheim, J. H.; Nair, M. G. Inhibition of Human Dihydrofolate Reductase by Antifolyl-Polyglutamates. *Biochem. Pharmacol.* **1989**, *38*, 541−543. (c) Rosowsky, A.; Galivan, J.; Beardsley, G. P.; Bader, H.; O'Connor, B. M.; Russello, O.; Moroson, B. A.; De Yarman, M. T.; Kerwar, S. S.; Freisheim, J. H. Biochemical and Biological Studies on 2-Desamino-2-methylaminopterin (dmAMT), an Antifolate the Polyglutamates of Which Are More Potent Than the Monoglutamates against Three Key Enzymes of Folate Metabolism. *Cancer Res.* **1992**, *52*, 2148−2155.

(19) (a) Rhee, M. S.; Wang, Y.; Nair, M. G.; Galivan, J. Acquisition of Resistance to Antifolates Caused by Enhanced γ-Glutamyl Hydrolase Activity. *Cancer Res.* **1993**, *53*, 2227−2230. (b) Yao, R.; Rhee, M. S.; Galivan, J. Effects of γ-Glutamyl Hydrolase on Folyl and Antifolyl Polyglutamates in Cultured Rat Hepatoma Cells. *Mol. Pharmacol.* **1995**, *48*, 505−511. (c) Rots, M. G.; Pieters, R.; Peters, G. J.; Noordhuis, P.; van Zantwijk, C. H.; Kaspers, G. J. L.; Hahlen, K.; Creutzig, U.; Veerman, A. J. P.; Jansen G. Role of Folylpolyglutamate Synthetase and Folylpolyglutamate Hydrolase in Methotrexate Accumulation and Polyglutamylation in Childhood Leukemia. *Blood* **1999**, *93*, 1677−1683. (d) Cole, P. D.; Kamen, B. A.; Gorlick, R.; Banerjee, D.; Smith, A. K.; Magill, E.; Bertino, J. R. Effects of Overexpression of γ-Glutamyl Hydrolase on Methotrexate Metabolism and Resistance. *Cancer Res.* **2001**, *61*, 4599−4604.

(20) (a) Hooijberg, J. H.; Broxterman, H. J.; Kool, M.; Assaraf, Y. G.; Peters, G. J.; Noordhuis, P.; Scheper, R. J.; Borst, P.; Pinedo, H. M.; Jansen, G. Antifolate Resistance Mediated by the Multidrug Resistance Proteins MRP1 and MRP2. *Cancer Res.* **1999**, *59*, 2532−2535. (b) Zeng, H.; Chen, Z. S.; Belinsky, M. G.; Rea, P. A.; Kruh, G. D. Transport of Methotrexate (MTX) and Folates by Multidrug Resistance Protein (MRP) 3 and MRP1: Effect of Polyglutamylation on MTX Transport. *Cancer Res.* **2001**, *61*, 7225−7232. (c) Chen, Z. S.; Lee, K.; Walther, S.; Raftogianis, R. B. Kuwano, M.; Zeng, H.; Kruh, G. D. Analysis of Methotrexate and Folate Transport by Multidrug Resistance Protein 4 (ABCC4): MRP4 Is a Component of the Methotrexate Efflux System. *Cancer Res.* **2002**, *62*, 3144−3150.

JM040122S